

Coherent control in quantum open systems: An approach for accelerating dissipation-based quantum state generation

Ye-Hong Chen^{1,2}, Zhi-Cheng Shi^{1,2}, Jie Song³, Yan Xia^{1,2,*}, and Shi-Biao Zheng^{1,2}

¹*Department of Physics, Fuzhou University, Fuzhou 350116, China*

²*Fujian Key Laboratory of Quantum Information and Quantum Optics (Fuzhou University), Fuzhou 350116, China*

³*Department of Physics, Harbin Institute of Technology, Harbin 150001, China*

In this paper, we propose an approach to accelerate the dissipation dynamics for quantum state generation. The strategy is to add target-state-related coherent control fields into the dissipation process to intuitively improve the evolution speed. By applying the current approach, without losing the advantages of dissipation dynamics, the target stationary states can be generated in a much shorter time as compared to that via traditional dissipation dynamics. As a result, the current approach containing the advantages of coherent unitary dynamics and dissipation dynamics allows for significant improvement in quantum state generation.

PACS numbers: 03.67. Pp, 03.67. Mn, 03.67. HK

Keywords: Acceleration; Dissipation dynamics; Quantum state generation

For years, quantum dissipation has been treated as a resource rather than as a detrimental effect to generate a quantum state [1–7] in quantum open systems modeled by the Lindblad-Markovian master equation [8] ($\hbar = 1$)

$$\begin{aligned}\dot{\rho} &= -i[H_0, \rho] + \mathcal{L}\rho, \\ \mathcal{L}\rho &= \sum_k L_k \rho L_k^\dagger - \frac{1}{2}(L_k^\dagger L_k \rho + \rho L_k^\dagger L_k),\end{aligned}\quad (1)$$

where the overdot stands for a time derivative and L_k are the so-called Lindblad operators. By using dissipation, one can generate high-fidelity quantum states without accurately controlling the initial state or the operation time (usually, the longer the operation time is, the higher is the fidelity). Besides, dissipation dynamics is shown to be robust against parameter (instantaneous) fluctuations [1]. Due to these advantages, many schemes [9–21] have been proposed for dissipation-based quantum state generation in recent years based on different physical systems.

Generally speaking, to generate quantum states by quantum dissipation, the key point is to find (or design) a unique stationary state (marked as $|S\rangle$) which can not be transferred to other states while other states can be transferred to it. That is, the reduced system should satisfy

$$H_0|M\rangle \neq 0, H_0|S\rangle = 0, \tilde{L}_k^\dagger|S\rangle \neq 0, \tilde{L}_k|S\rangle = 0, \quad (2)$$

where $|M\rangle$ ($M \neq S$) are the orthogonal partners of the state $|S\rangle$ in a reduced system satisfying $\langle M|S\rangle = 0$ and $\sum_M |M\rangle\langle M| + |S\rangle\langle S| = \mathbf{1}$, and \tilde{L}_k are the effective Lindblad operators. Hence, if the system is in $|M\rangle$, it will always be transferred to other states because $H_0|M\rangle \neq 0$ and $\tilde{L}_k^\dagger|S\rangle \neq 0$, while if the system is in $|S\rangle$, it remains invariant. Therefore, the process of pumping and decaying continues until the system is finally stabilized into the stationary state $|S\rangle$.

To show such a dissipation process in more detail, we introduce a function \dot{V} to describe the system evolution speed, where $V = \text{Tr}(\rho\rho_s)$ and ρ_s is the density matrix of the target state $|S\rangle$. Hence, when the system evolves into a target state at a final time t_f , i.e., $\rho|_{t=t_f} \rightarrow \rho_s$, V approaches a maximum value $V = 1$. Based on Eqs. (1) and (2), we find

$$\dot{V} = \text{Tr}[-i[H_0, \rho] + \mathcal{L}\rho]\rho_s = \sum_k \Gamma_k \langle E_k|\rho|E_k\rangle \geq 0, \quad (3)$$

in which we have assumed $\tilde{L}_k = \sqrt{\Gamma_k}|S\rangle\langle E_k|$, with Γ_k being the effective dissipation rates and $|E_k\rangle$ being the effective excited states. Obviously, the evolution speed strongly depends on the effective dissipation rates and the total population of effective excited states. Hence, according to the dissipation dynamics, we have $\langle E_k|\rho|E_k\rangle \rightarrow 0$ when $t \rightarrow \infty$, which means $\dot{V}|_{t \rightarrow \infty} = 0$.

However, as is known, such a process is generally much slower than a unitary evolution process because of the small effective dissipation rates. It would be a serious issue to realize large-scale integrated computation if it takes too long to generate the desired quantum states. In view of this, the preponderance of dissipation-based approaches would lose if a future technique would present an ideal dissipation-free system. Therefore, accelerating the dissipation dynamics without losing its advantages should signal a significant improvement for quantum computation. Now that a unitary evolution process is much faster than a dissipation process, we are guided to ask, is it possible to accelerate the dissipation dynamics by using coherent control fields? In this paper, we will answer this question by seeking additional coherent control fields which behave very well in accelerating dissipation dynamics.

The strategy of accelerating dissipation dynamics is to add a simple and realizable coherent control Hamiltonian H_c to increase the value of \dot{V} in Eq. (3). The state evolution equation in this case becomes

$$\dot{\rho} = -i[H_0 + H_c, \rho] + \mathcal{L}\rho, \quad (4)$$

*E-mail: xia-208@163.com

where $H_c = \sum_n f_n(t)H_n$ is the additional control Hamiltonian, H_n are time independent, and control functions $f_n(t)$ are realizable and real valued. The corresponding evolution speed reads

$$\begin{aligned} \dot{V}_a = & \text{Tr}[-i[H_0, \rho] + \mathcal{L}\rho]\rho_s] \\ & + \sum_n f_n(t)\text{Tr}[-i[H_n, \rho]]\rho_s]. \end{aligned} \quad (5)$$

We use the symbol \dot{V}_a to distinguish from the original evolution speed \dot{V} . The control functions $f_n(t)$ should be carefully chosen to ensure that $V_a|_{t=t_f} = 1$ and $\dot{V}_a|_{t=t_f} = 0$. For this goal, the simplest choice for $f_n(t)$ is

$$f_n(t) = \text{Tr}[-i[H_n, \rho]]\rho_s. \quad (6)$$

As can be seen from Eq. (2), the Hamiltonian H_0 is just used to ensure that $|S\rangle$ is a stationary state, while, by adding additional coherent fields, it is easy to find $(H_0 + H_c)|S\rangle \neq 0$ (for $\rho \neq \rho_s$ corresponding to $t < t_f$), which means $|S\rangle$ is actually not a stationary state when $t < t_f$. For $t \rightarrow t_f$, according to Eq. (6), we have $f_n(t_f) = 0$ since $\rho|_{t=t_f} \rightarrow \rho_s$. Thus, $H_c = 0$, so that $|S\rangle$ becomes a unique stationary state when $t = t_f$. That is, when $t < t_f$, the coherent fields and dissipation work together to drive the system to state $|S\rangle$, while when $t \rightarrow t_f$, the additional coherent fields vanish and the system becomes steady. It can also be understood as, in the current approach, $|S\rangle$ is not a stationary state until the population is totally transferred to it. Obviously, such a process is significantly different from the previous dissipation-based schemes [1, 14–18], in which $|S\rangle$ is the unique stationary state during the whole evolution.

Usually, part of H_0 can be chosen as H_n to make sure that H_n is realizable. In this case, the additional coherent control fields can be actually regarded as a modification on Hamiltonian H_0 . So, the current approach can be actually understood as a parameter optimization approach for dissipation-based quantum state generation. In the following, we will verify the accelerating approach with applications to quantum state generation.

Application I: Single-atom superposition state. We first consider a three-level Λ atom with an excited state $|e\rangle$ and two ground states $|g_1\rangle$ and $|g_2\rangle$ to illustrate our accelerating approach. The transition $|e\rangle \leftrightarrow |g_{1,(2)}\rangle$ is resonantly driven by a laser field with a Rabi frequency $\Omega_{1,(2)}$. The Hamiltonian in the interaction picture is thus written as $H_0 = \Omega_0(\sin\theta|e\rangle\langle g_1| + \cos\theta|e\rangle\langle g_2|) + H.c.$, where $\Omega_0 = \sqrt{\Omega_1^2 + \Omega_2^2}$ and $\theta = \arctan \frac{\Omega_1}{\Omega_2}$. The Lindblad operators in this Λ system associated with atomic spontaneous emission are $L_1 = \sqrt{\gamma_1/2}|g_1\rangle\langle e|$ and $L_2 = \sqrt{\gamma_2/2}|g_2\rangle\langle e|$, respectively. Then, we introduce the orthogonal states $|S\rangle = \cos\varphi|g_1\rangle - \sin\varphi|g_2\rangle$ and $|T\rangle = \sin\varphi|g_1\rangle + \cos\varphi|g_2\rangle$ to rewrite the Hamiltonian H_0 as $H_0 = \Omega_S|e\rangle\langle S| + \Omega_T|e\rangle\langle T| + H.c.$, where $\Omega_S = \Omega_0 \sin(\theta - \varphi)$ and $\Omega_T = \Omega_0 \cos(\theta - \varphi)$. Accordingly, by choosing $\gamma_1 = \gamma_2 = \gamma$, we obtain two effective Lindblad operators $\tilde{L}_S = \sqrt{\gamma/2}|S\rangle\langle e|$ and $\tilde{L}_T = \sqrt{\gamma/2}|T\rangle\langle e|$. It is

clear that if we choose $\theta = \varphi$, the effective driving field between $|e\rangle$ and $|S\rangle$ with a Rabi frequency Ω_S will be switched off and the condition in Eq. (2) will be satisfied. In this case, according to dissipation dynamics, the system will be stabilized into the stationary state $|S\rangle$.

By choosing $t_f = 10/\Omega_0$, the evolution speed \dot{V} and time-dependent population for state $|S\rangle$ versus γ are displayed in Figs. 1 (a) and (b), respectively. As shown in the figure, to obtain the target state $|S\rangle$ in a relatively high fidelity ≥ 0.95 within a fixed evolution time $t_f = 10/\Omega_0$, the decay rate should be at least $\gamma \geq \Omega_0$ ($P_S|_{t=t_f} = 0.9506$ when $\gamma = \Omega_0$). To accelerate such a process by additional coherent control fields, we choose the control Hamiltonians H_n as $H_1 = \mu_1|e\rangle\langle g_1| + H.c.$ and $H_2 = \mu_2|e\rangle\langle g_2| + H.c.$, where μ_1 and μ_2 are two arbitrary time-independent parameters used to control the intensities of the control fields. By choosing $\mu_1 = 0.8$ and $\mu_2 = 0.6$ as an example, the optimized evolution speed \dot{V}_a given according to Eq. (5) is shown in Fig. 1 (c). Contrasting Figs. 1 (c) with (a), it is clear that the evolution speed has been significantly improved, especially, when the decay rate γ is relatively small. For example, when $\gamma = 0.5\Omega_0$, the maximum value of the evolution speed has been increased from $\dot{V}^{max} \approx 0.08$ to $\dot{V}_a^{max} \approx 0.26$. While for a relatively large decay rate, the increasing effect is relatively weak. This is because the control functions $f_n(t)$ are mainly decided by the instantaneous distance $d = 1 - \text{Tr}(\rho\rho_s)$ from the target state according to Eq. (6). In general, $f_n(t)$ are in direct proportion to d . In a certain period of time, more population will be transferred to the stationary state $|S\rangle$ with a relatively large decay rate (see Fig. 1). That is,

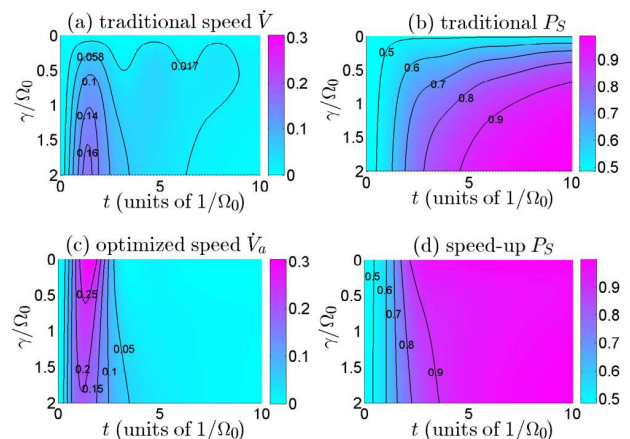


FIG. 1: Single-atom superposition state preparation: The comparison with respect to the evolution speed between the traditional dissipation dynamics and the accelerated dissipation dynamics. (a) and (c): The evolution speeds given according to Eq. (3) and Eq. (5) versus γ , respectively. (b) and (d): The time-dependent populations governed by the traditional dissipation dynamics and the accelerated dissipation dynamics, respectively.

the instantaneous value of $\text{Tr}(\rho\rho_s)$ decreases with the increase of γ . Accordingly, the control functions $f_n(t)$ will fade away along with the increase of the decay rate γ . To show the fidelity of the accelerated state generation in more detail, we display the fidelity of the target state $|S\rangle$ versus operation time $\mathcal{T} = t_f - t_i$ ($t_i = 0$ is the initial time) and decay rate γ in Fig. 2 (a). For clarity, in the following, we will use the symbols \mathcal{T}_t and \mathcal{T}_a to express operation times via traditional dissipation dynamics and accelerated dissipation dynamics, respectively. It is clear from Fig. 2 (a) that the efficiency of state generation has been remarkably improved since a relatively high fidelity ($F_S \approx 0.95$) of the target state $|S\rangle$ can be achieved even when the operation time is only $\mathcal{T}_a = 5/\Omega_0$. The shapes for the additional control fields are shown to be smooth curves [see Fig. 2 (b) with $\gamma = 0.8\Omega_0$ as an example] which can be easily realized in practice. For example, one can use electrooptic modulators to implement such coherent fields.

Affected by the real experimental environment, there is usually a stochastic kind of noise that should be considered in realizing the scheme. Assume that the Hamiltonian H_0 is perturbed by some stochastic part ηH_s describing amplitude noise. A stochastic Schrödinger equation in a closed system (in the Stratonovich sense) is then $\dot{\psi}(t) = [H_0 + \eta H_s \xi(t)]\psi(t)$, where $\xi(t) = \partial_t W_t$ is heuristically the time derivative of the Brownian motion W_t . $\xi(t)$ satisfies $\langle \xi(t) \rangle = 0$ and $\langle \xi(t)\xi(t') \rangle = \delta(t - t')$ because the noise should have zero mean and the noise at different times should be uncorrelated. Then, we define $\rho_\xi(t) = |\psi_\xi(t)\rangle\langle\psi_\xi(t)|$, and the dynamical equation without dissipation for ρ_ξ is thus given as

$$\dot{\rho}_\xi = -i[H_0, \rho_\xi] - i\eta[H_s, \xi\rho_\xi]. \quad (7)$$

After averaging over the noise, Eq. (7) becomes $\dot{\rho} \simeq -i[H_0, \rho] - i\eta[H_s, \langle \xi\rho_\xi \rangle]$, where $\rho = \langle \rho_\xi \rangle$ [22]. According to Novikov's theorem in the case of white noise, we have $\langle \xi\rho_\xi \rangle = \frac{1}{2} \langle \frac{\delta\rho_\xi}{\delta\xi(t')} \rangle|_{t'=t} = -\frac{i\eta}{2}[H_s, \rho]$. Hence, when both the amplitude noise and dissipation are considered, the

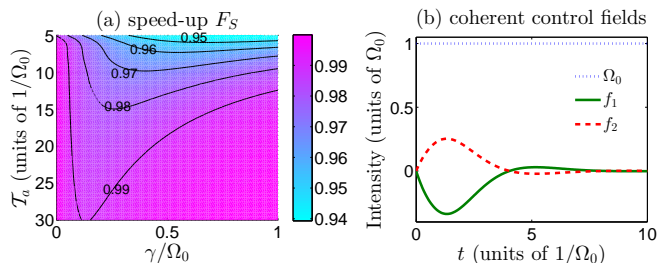


FIG. 2: Single-atom superposition state preparation: (a) Fidelity F_S of the accelerated dissipation scheme versus \mathcal{T}_a and γ , where the fidelity F_S is defined by $F_S = \langle S|\rho|S\rangle|_{t=t_f}$ expressing the final population for the target state. (b) The coherent control fields for the accelerated dissipation scheme when $\gamma = 0.8\Omega_0$. In general, the intensity for the additional coherent control fields should be smaller than $\Omega_{1,(2)}$.

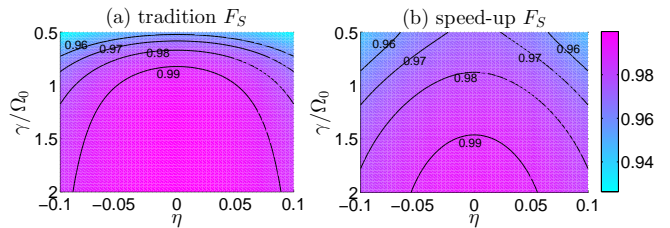


FIG. 3: Single-atom superposition state preparation: The comparison with respect to the robustness against amplitude-noise error between the traditional dissipation dynamics and the accelerated dissipation dynamics. (a) F_S versus η and γ via traditional dissipation dynamics with $\mathcal{T}_t = 20/\Omega_0$. (b) F_S versus η and γ via the accelerated dissipation dynamics with $\mathcal{T}_a = 10/\Omega_0$. Here $\mathcal{T}_a = 10/\Omega_0$ is chosen to make the highest fidelity for each γ in Fig. 3 (b) to be the same as that in Fig. 3 (a) as far as possible.

dynamics of the open system will be governed by

$$\dot{\rho} \simeq -i[H_0, \rho] + \mathcal{N}\rho + \mathcal{L}\rho, \quad (8)$$

where $\mathcal{N}\rho = -\frac{\eta^2}{2}[H_s, [H_s, \rho]]$.

For the current three-level scheme, we consider an independent amplitude noise in Ω_1 as well as in Ω_2 with the same intensity η^2 , and the noise term in Eq. (8) is thus

$$\mathcal{N}\rho = -\frac{\eta^2}{2}([H_{s1}, [H_{s1}, \rho]] + [H_{s2}, [H_{s2}, \rho]]), \quad (9)$$

where $H_{s1} = \Omega_1|e\rangle\langle g_1| + H.c.$ and $H_{s2} = \Omega_2|e\rangle\langle g_2| + H.c.$. According to Eq. (8), the robustness against amplitude-noise error for the dissipation-based state generation without the additional coherent control fields is shown in Fig. 3 (a), in which the operation time is chosen as $\mathcal{T}_t = 20/\Omega_0$. Only a $\sim 2\%$ deviation will occur in the fidelity as shown in the figure with a relatively small decay rate $\gamma \leq 1$ and the noise intensity is $\eta = 0.1$. The robustness of the scheme against amplitude-noise error is better when the decay rate gets larger. For comparison, the robustness against the amplitude-noise error of the accelerated dynamics governed by $\dot{\rho} \simeq -i[H_0 + H_c, \rho] + \mathcal{N}\rho + \mathcal{L}\rho$, is shown in Fig. 3 (b) with operation time $\mathcal{T}_a = 10/\Omega_0$. The result shows the robustness of the accelerated scheme with respect to amplitude-noise error is almost the same with that of the traditional scheme. A stochastic noise with intensity $\eta = 0.1$ also causes a deviation of about 2% on the fidelity when $\gamma \leq 1$, and the influence of noise decreases with increasing γ . That is, we have confirmed that the approach by adding coherent control fields can realize the goal of accelerating the dissipation process without losing the advantage of robustness against parameter fluctuations.

Application II: two-atom entanglement. We consider two Λ atoms with a level structure, as shown in Fig. 4 (a) (marked as atom A and atom B), which are trapped in an optical cavity. The transition $|g_1\rangle_m \leftrightarrow |e\rangle_m$ ($m = A, B$) is resonantly driven by a laser with Rabi frequency Ω_m ,

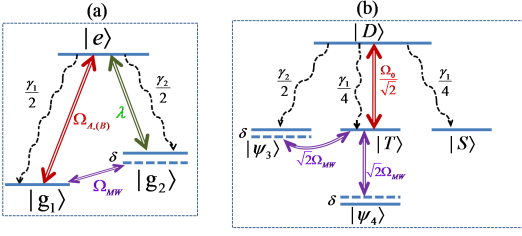


FIG. 4: Two-atom entanglement preparation: (a) Level diagram of a single atom. The optical pumping laser for the two atoms differs by a relative phase of π . (b) The effective transitions for two-atom trapped system. With the effective driving fields and decays, ultimately, the system will be stabilized into the state $|S\rangle$.

and the transition $|g_2\rangle_m \leftrightarrow |e\rangle_m$ is coupled to the quantized cavity field resonantly with coupling strength λ . Besides, we apply a microwave field with Rabi frequency Ω_{MW} to drive the transition between ground states $|g_1\rangle_m$ and $|g_2\rangle_m$ with detuning δ . The Hamiltonian for this system in an interaction picture reads

$$H_0 = \sum_{m=A,B} \Omega_m |e\rangle_m \langle g_1| + \Omega_{MW} e^{i\delta t} |g_2\rangle_m \langle g_1| + \lambda |e\rangle_m \langle g_2| a + H.c., \quad (10)$$

where a denotes the cavity annihilation operator. The corresponding dynamics of the current system is described by the master equation in Eq. (1). The Lindblad operators associated with atomic spontaneous emission and cavity decay are $L_{m_1} = \sqrt{\gamma_1/2} |g_1\rangle_m \langle e|$, $L_{m_2} = \sqrt{\gamma_2/2} |g_2\rangle_m \langle e|$ ($m = A, B$), and $L_C = \sqrt{\kappa} a = \sqrt{\kappa} |0\rangle_C \langle 1|$, where κ is the cavity decay rate and $|k\rangle_C$ ($k = 0, 1$) denotes the photon number in the cavity.

Referring to the formula of quantum Zeno dynamics [23], we write the Hamiltonian H_0 as $H_0 = \Omega(H_p + KH_q)$, where $\Omega = \sqrt{\Omega_A^2 + \Omega_B^2 + \Omega_{MW}^2}$, $K = g/\Omega$, H_p stands for the dimensionless interaction Hamiltonian between the atom and the classical field, and H_q denotes the counterpart between the atom and the quantum cavity field. When the strong coupling limit $K \rightarrow \infty$ is satisfied, we obtain the effective Hamiltonian $H_0^{eff} = \Omega_a(\sum_l P_l H_p P_l + K \epsilon_l P_l)$, where P_l is the eigenprojection and ϵ_l is the corresponding eigenvalue of H_q : $H_q = \sum_l \epsilon_l P_l$. Assuming the system is initially in the Zeno dark subspace ($\epsilon_l = 0$) spanned by $|\psi_1\rangle = |g_1 g_2\rangle_{A,B} |0\rangle_C$, $|\psi_2\rangle = |g_2 g_1\rangle_{A,B} |0\rangle_C$, $|\psi_3\rangle = |g_2 g_2\rangle_{A,B} |0\rangle_C$, $|\psi_4\rangle = |g_1 g_1\rangle_{A,B} |0\rangle_C$, and $|D\rangle = \frac{1}{\sqrt{2}}(|e g_2\rangle_{A,B} - |g_2 e\rangle_{A,B}) |0\rangle_C$, the effective Hamiltonian reduces to ($\Omega_A = -\Omega_B$ and $\Omega_0 = \sqrt{\Omega_A^2 + \Omega_B^2}$)

$$H_0^{eff} = \frac{\Omega_0}{\sqrt{2}} |D\rangle \langle T| + \sqrt{2} \Omega_{MW} e^{i\delta t} |\psi_3\rangle \langle T| + \sqrt{2} \Omega_{MW} e^{-i\delta t} |\psi_4\rangle \langle T| + H.c., \quad (11)$$

where $|S\rangle = (|\psi_1\rangle - |\psi_2\rangle)/\sqrt{2}$ and $|T\rangle = (|\psi_1\rangle + |\psi_2\rangle)/\sqrt{2}$. Accordingly, the effective Lindblad operators are $\tilde{L}_G = \sqrt{\gamma_2/2} |\psi_3\rangle \langle D|$, $\tilde{L}_S = \sqrt{\gamma_1/4} |S\rangle \langle D|$, and

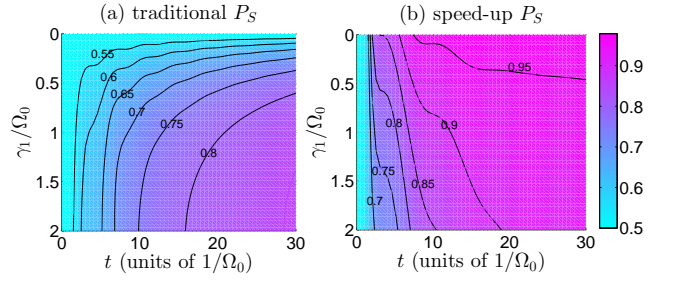


FIG. 5: Two-atom entanglement preparation: The comparison with respect to the two-atom entanglement generation between the traditional dissipation dynamics and the accelerated dissipation dynamics. (a) P_S versus γ_1 via traditional dissipation dynamics. (b) P_S versus γ_1 via accelerated dissipation dynamics. The basic parameters in plotting the figure are $\lambda = 10\Omega_0$, $\delta = 0.15\Omega_0$, $\kappa = 0.5\Omega_0$, $\gamma_2 = 0.5\gamma_1$, and $\Omega_{MW} = 0.2\Omega_0$. The initial state is selected as $\rho_0 = |\psi_1\rangle \langle \psi_1|$.

$\tilde{L}_T = \sqrt{\gamma_1/4} |T\rangle \langle D|$. The cavity field has been decoupled in the effective Hamiltonian when the Zeno condition is satisfied thus the cavity decay can be neglected. Figure 4 (b) shows the effective transitions of reduced system.

The time-dependent population for the target state $|S\rangle$ versus decay rate γ_1 is shown in Fig. 5 (a). Obviously, an operation time $\mathcal{T}_t = 30/\Omega_0 = 300/\lambda$ is not enough to generate the entangled state $|S\rangle$ [the maximum population for $|S\rangle$ in Fig. 3 (a) is only 0.8548]. A further study shows that for $\gamma_1 \leq 2\Omega_0$, an operation time $\mathcal{T}_t \geq 1000/\lambda = 100/\Omega_0$ is necessary in order to obtain a relatively high-fidelity ($F_S \geq 0.9$) entanglement. Such results can be also found in the previous schemes for the generation of two-atom entanglement. For example, in Ref. [1], by choosing parameters similar to those in plotting Fig. 5 (a), the time required for entanglement generation with fidelity $F_S \geq 0.9$ is $\mathcal{T}_t \geq 1300/\lambda = 130/\Omega_0$. The control Hamiltonians to accelerate entanglement generation are chosen as $H_1 = \mu_1 |e\rangle_A \langle g_1| + H.c.$ and $H_2 = \mu_2 |e\rangle_B \langle g_1| + H.c.$. We randomly select $\mu_1 = 1$ and $\mu_2 = 1.5$ as an example to show time-dependent P_S versus γ_1 in Fig. 5 (b). One can find from Fig. 5 that the entanglement generation has been accelerated by the additional coherent control fields. An operation time $\mathcal{T}_a \leq 20/\Omega_0$ is enough to generate two-atom entanglement with fidelity $F_S \geq 0.9$. In fact, by choosing suitable parameters for a specified decay rate, the fidelity can be further improved (See Fig. 6). As shown in the figure, for decay rate $\gamma_1 = 0.5\Omega_0$ [See Fig. 6 (a)], the optimal parameters are $\delta = 0$ and $\Omega_{MW} \sim 0.25\Omega_0$, and the corresponding fidelity is $F_S \sim 0.97$; for decay rate $\gamma_1 = \Omega_0$ [See Fig. 6 (b)], when $\delta \sim 0.6\Omega_0$ and $\Omega_{MW} \sim 0.15\Omega_0$, we have the highest fidelity $F_S \sim 0.96$; for decay rate $\gamma_1 = 2\Omega_0$ [See Fig. 6 (c)], the highest fidelity $F_S \sim 0.96$ appears when $\delta \sim 0.5\Omega_0$ and $\Omega_{MW} \sim 0.2\Omega_0$. The experimentally achievable values for cooperativity are around $C = \lambda^2/(\gamma_1 \kappa) \approx 100$ [24], corresponding to $\gamma_1 \approx 2\Omega_0$ and $\kappa \approx 0.5\Omega_0$. For $\lambda = (2\pi)35\text{MHz}$, with the experimentally

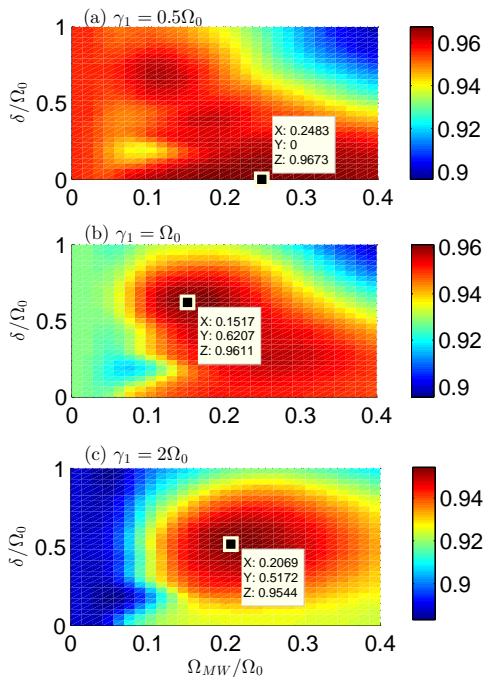


FIG. 6: Two-atom entanglement preparation: The fidelity F_S versus detuning δ and Rabi frequency Ω_{MW} with (a) $\gamma_1 = 0.5\Omega_0$; (b) $\gamma_1 = \Omega_0$; (c) $\gamma_1 = 2\Omega_0$. The basic parameters in plotting the figure are $\lambda = 10\Omega_0$, $\kappa = 0.5\Omega_0$, and $\gamma_2 = 0.5\gamma_1$. The initial state is selected as $\rho_0 = |\psi_1\rangle\langle\psi_1|$.

achievable parameters, the operation time required for the entanglement generation is only about $1.3 \mu\text{s}$, which is much shorter than the typical decoherence time scales for this system.

In conclusion, we have investigated the possibility of accelerating dissipation-based state generation in a three-level system and a trapped two-atom system. From both analytical and numerical evidence, we have shown that the speed for a system to reach the target state has been significantly improved with additional coherent control fields, without losing the advantage of robustness against parameter fluctuations. Notably, the additional control fields are given basically according to the definition of the system evolution speed via dissipation dynamics [see Eq. (3)], while there are in fact other definitions that can be used and the control fields would be accordingly changed. So, in the future, it would be interesting to study the behavior of the given additional coherent control fields based on other definitions of the evolution speed.

This work was supported by the National Natural Science Foundation of China under Grants No. 11575045, No. 11374054 and No. 11674060.

-
- [1] M. J. Kastoryano, F. Reiter, and A. S. Sørensen, Phys. Rev. Lett. **106**, 090502 (2011).
 [2] X. T. Wang and S. G. Schirmer, arXiv: 1005.2114v2 (2010).
 [3] G. Vacanti and A. Beige, New J. Phys. **11**, 083008 (2009).
 [4] R. Blatt and D. Wineland, Nature **453**, 1008 (2008).
 [5] B. Baumgartner, H. Narnhofer, W. Thirring, J. Phys. A **41**, 065201 (2008).
 [6] F. Verstraete, M. M. Wolf, and J. I. Cirac, Nature Phys. **5**, 633 (2009).
 [7] K. G. H. Vollbrecht, C. A. Muschik, and J. I. Cirac, Phys. Rev. Lett. **107**, 120502 (2011).
 [8] G. Lindblad, Commun. Math. Phys. **48**, 119 (1976).
 [9] F. Reiter, M. J. Kastoryano, and A. S. Sørensen, arXiv:1110.1024v1 (2012).
 [10] D. Braun, Phys. Rev. Lett. **89**, 277901 (2002).
 [11] L. Memarzadeh and S. Mancini, Phys. Rev. A **83**, 042329 (2011).
 [12] A. F. Alharbi and Z. Ficek, Phys. Rev. A **82**, 054103 (2010).
 [13] J. Busch, S. De, S. S. Ivanov, B. T. Torosov, T. P. Spiller, and A. Beige, Phys. Rev. A **84**, 022316 (2011).
 [14] X. L. Wang, *et al.*, Phys. Rev. Lett. **117**, 210502 (2016).
 [15] L. T. Shen, X. Y. Chen, Z. B. Yang, H. Z. Wu, and S. B. Zheng, Phys. Rev. A **84**, 064302 (2011).
 [16] Y. Lin, *et al.*, Nature **504**, 415 (2013).
 [17] A. W. Carr and M. Saffman, Phys. Rev. Lett. **111**, 033607 (2013).
 [18] X. Q. Shao, J. H. Wu, and X. X. Yi, Phys. Rev. A **95**, 022317 (2017).
 [19] A. Neuzner, M. Körber, O. Morin, S. Ritter, and G. Rempe, Nature Photonics **10**, 303 (2016).
 [20] F. Reiter, D. Reeb, and A. S. Sørensen, Phys. Rev. Lett. **117**, 040501 (2016).
 [21] G. Morigi, J. Eschner, C. Cormick, Y. Lin, D. Leibfried, and D. J. Wineland, Phys. Rev. Lett. **115**, 200502 (2015).
 [22] A. Ruschhaupt, X. Chen, D. Alonso, and J. G. Muga, New J. Phys. **14**, 093404 (2014).
 [23] P. Facchi and S. Pascazio, Phys. Rev. Lett. **89**, 080401 (2002); J. Phys. A **41**, 493001 (2008).
 [24] A. D. Boozer, A. Boca, R. Miller, T. E. Northup, and H. J. Kimble, Phys. Rev. Lett. **97**, 083602 (2006); K. Hennessy, *et al.*, Nature **445**, 896 (2007).